Theoretical Study on the Pyrolysis of Sulphonyl Oximes in the Gas Phase

Ying Xue, Kyung A Lee, and Chan Kyung Kim*

Department of Chemistry, Inha University, Inchon 402-751, Korea
Received February 28, 2003

The reaction mechanism of the pyrolysis of sulphonyl oximes (CH_3-C_6H_4-$S(O)_2O$-N=C(H)-C_6H_4Y), in the gas phase is studied theoretically at HF/3-21G, ONIOM (B3LYP/6-31G**:HF/3-21G) and ONIOM (MP2/6-31G**:HF/3-21G) levels. All the calculations show that the thermal decomposition of sulphonyl oximes is a concerted asynchronous process *via* a six-membered cyclic transition state. The activation energies (Ea) predicted by ONIOM (B3LYP/6-31G**: HF/3-21G) method are in good agreement with the experimental results for a series of tosyl arenecarboxaldoximes. Five para substituents, Y = OCH_3, CH_3, H, Cl, and NO_2, are employed to investigate the substituent effect on the elimination reaction. Linear Hammett correlations are obtained in all calculations in contrast to the experimental finding.

Key Words : Sulphonyl oximes, Pyrolysis, ONIOM method, Transition state, Substituent effect

Introduction

The sulphonic acids and cyanoarene compounds are the products of the pyrolysis of sulphonyl oximes, which are important in biomedical and industrial applications. The experimental investigations have been performed to study the kinetics and mechanism of the thermal decomposition of sulphonyl hydrazones and oximes in gas phase.[1,2] Some similar reactions have also been studied for 3-phenylhydrazonopentane-2,4-dione,[3] ethyl (hetero) arylcarboxylate esters,[4] and heterocyclic hydrazone[5] systems experimentally. The common character of these reactions is that they were found to be homegeneous and unimolecular, and follow first-order rate law. The Arrhenius parameters, Hammett correlations, and analysis of reaction products suggested that these thermal gas-phase decomposition reactions proceeded through a concerted six-membered ring transition state. The elimination pathway of a series of arenesulphonyl arenecarboxaldoximes is described in Scheme 1.

The experimental results have shown that molecular reactivity in the oxime compounds is dominated by the greater polarity of the N-O σ-bond (bond (a) in Scheme 1) but the rate constants do not exhibit any such trend with respect to the para substituents Y in benzene ring.[2]

In this work, we theoretically study the molecular mechanism of the pyrolysis of sulphonyl oximes (Y = OCH_3, CH_3, H, Cl, NO_2) in gas phase using HF/3-21G, ONIOM methods. The effects of substituent in Y-ring on the reactivity of these oximes are investigated.

Computational Details

It is well known that high level of theory and large basis set are needed for the calculations of activation energies and geometries of transition states in chemical reactions. For large reaction system, however, highly accurate calculation including electron correlation has become very expensive and difficult. Because the molecules participating in the reactions in the present study are relatively large, an *ab initio* MO HF method with 3-21G basis set was chosen. We also employed two two-layered ONIOM method[6,7] to calculate the optimized geometries, energies, and molecular properties.

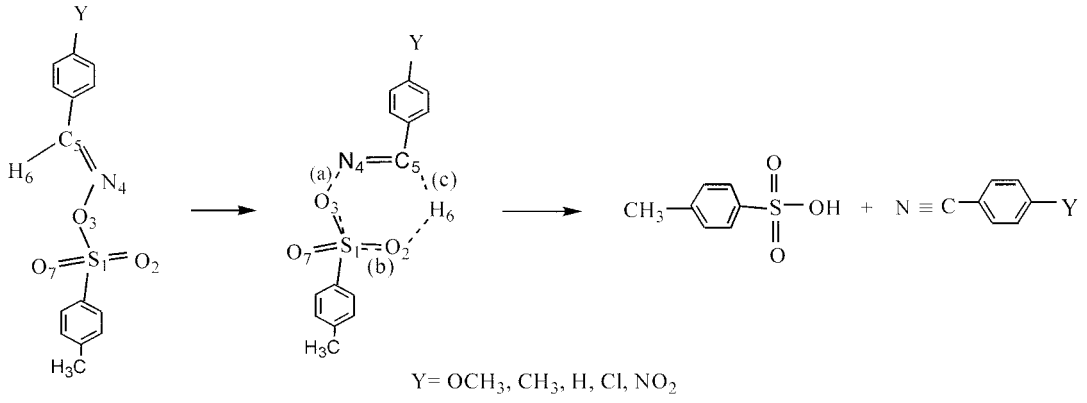

Y= OCH_3, CH_3, H, Cl, NO_2

Scheme 1

*To whom correspondence should be addressed. E-mail: kckyung@inha.ac.kr

in which molecule was divided into two layers: the inner or high layer was treated either using Becke's three-parameter hybrid DFT method[8] with Lee-Yang-Parr's correlation functional[9] (B3LYP) or Möller-Plesset 2nd order perturbation theory (MP2) and the 6-31G** basis set.[10] and the rest of the system (the outer layer) was described by HF/3-21G level of theory. The ONIOM(B3LYP/6-31G**:HF/3-21G) and ONIOM (MP2/6-31G**:HF/3-21G) methods were abbreviated to ONIOM (DFT) and ONIOM (MP2), respectively. For all molecules in question, atoms S_1, O_2, O_3, N_4, C_5, H_6, and O_7 (see Scheme 1) were in the inner layer. All MO calculations were carried out with the Gaussian 98 program.[11]

The HF/3-21G and ONIOM methods were used to optimize geometric parameters of the reactants (RE), the transition states (TS), and the products (PR) for all the tosyl arenecarboxaldoximes (Y=OCH_3, CH_3, H, Cl, and NO_2). The harmonic vibrational frequencies of the optimized structures were calculated to confirm the stationary point as a local minima with all positive frequencies or as a transition state with only one imaginary frequency, and to provide the zero-point vibrational energy (ZPVE), absolute entropy, enthalpy and Gibbs free energy. The HF/3-21G results are not included in detail because they are similar to the ONIOM (MP2) results. An intrinsic reaction coordinate (IRC) calculation[12] was also performed at HF/3-21G level for TS of oxime to ensure it to connect to the desired reactant and product. The charges of atoms and groups in stationary points of oxime were calculated using natural population analysis. In this paper, all thermodynamic data were estimated at the experimental decomposition temperature of 380 K and pressure of 1.0 atm as presented in Ref. [2]. The theoretical activation energy E_a was calculated by Eq. (1):

$$E_a = \Delta H^{\neq} + RT \quad (1)$$

Results and Discussions

The experimental work reported by Al-Awadi *et al.*[2] suggested that the thermal elimination of oximes passes through a six-membered ring transition state irrespective of substituents and presented the reaction rate coefficients k and Arrhenius activation energies E_a for a series of sulphonyl oximes (Y = OCH_3, CH_3, H, and Cl). Discussions about the structures of stationary points on the potential energy surface, energetics, and nature of reaction mechanism in this study will be given for these compounds for the purpose of comparison. The reaction pathway is depicted in Scheme 1, in which the relevant atom numbering is also indicated.

Stationary Structures. The ONIOM fully optimized structures of reactant (RE), transition state (TS), and the corresponding products (PR1 and PR2) for tosyl arene-carboxaldoxime (Y=H) are depicted in Figure 1. Selected geometric parameters of the optimized reactant and transition state structures of all Y-ring-substituted tosyl arene-carboxaldoximes at ONIOM level are reported in Table 1.

The calculated equilibrium geometry of reactant has an extended structure as shown in Figure 1. This is due to the fact that the repulsive interaction between lone-pair electrons of O_3 and N_4 atoms is the smallest as they point towards the opposite directions. Atoms S_1, O_3, N_4, C_5, and H_6 are almost in a plane. It can be seen from Table 1 that the substituent on Y-ring does not change the structure of reactants significantly. Additionally, weak hydrogen bond between O_3 and H_6 atoms with O_3-H_6 distance of 2.34-2.36 Å stabilizes the structure.

Owing to such direction of H_6 atom, it is possible to form a

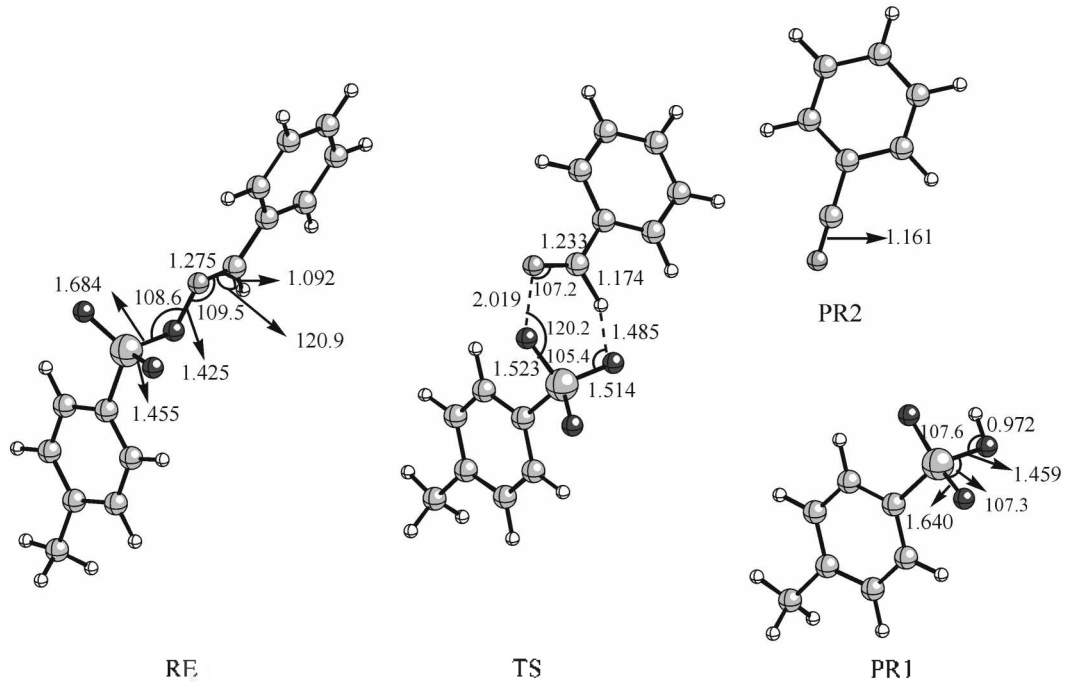

Figure 1. Optimized structures of reactant (RE), transition state (TS), p-methyl-benzenesulfonic aicd (PR1) and benzonitrile (PR2) at ONIOM (DFT) level of theory for oxime (Y=H).

Table 1. Selected set of optimized geometric parameters of the reactants (RE) and transition states (TS) for tosyl arenecarboxaldoximes (Y = OCH_3, CH_3, H, Cl, NO_2) at ONIOM (DFT) and ONIOM (MP2) levels[a,b]

Y	OCH_3		CH_3		H		Cl		NO_2	
	RE	TS	RE	TS	RE	TS	RE	TS	RE	TS
Bond length										
S_1=O_2	1.455	1.512	1.455	1.513	1.455	1.514	1.455	1.517	1.454	1.520
	(1.454)	(1.514)	(1.454)	(1.514)	(1.453)	(1.515)	(1.453)	(1.516)	(1.453)	(1.520)
S_1-O_3	1.681	1.523	1.682	1.523	1.684	1.523	1.691	1.524	1.700	1.525
	(1.675)	(1.531)	(1.677)	(1.531)	(1.679)	(1.532)	(1.684)	(1.533)	(1.692)	(1.531)
O_3-N_4	1.429	2.026	1.428	2.024	1.425	2.019	1.419	2.005	1.411	1.988
	(1.438)	(1.913)	(1.437)	(1.910)	(1.435)	(1.906)	(1.429)	(1.893)	(1.421)	(1.904)
N_4=C_5	1.276	1.237	1.276	1.234	1.275	1.233	1.274	1.232	1.273	1.229
	(1.288)	(1.229)	(1.287)	(1.227)	(1.287)	(1.227)	(1.286)	(1.226)	(1.285)	(1.222)
C_5-H_6	1.093	1.167	1.093	1.171	1.092	1.174	1.092	1.183	1.092	1.194
	(1.086)	(1.206)	(1.086)	(1.210)	(1.086)	(1.212)	(1.086)	(1.219)	(1.086)	(1.236)
S_1=O_7	1.455	1.457	1.455	1.456	1.455	1.456	1.455	1.455	1.454	1.454
	(1.454)	(1.449)	(1.454)	(1.449)	(1.453)	(1.449)	(1.453)	(1.448)	(1.453)	(1.447)
H_6-O_2	4.626	1.507	4.629	1.496	4.630	1.485	4.637	1.459	4.646	1.428
	(4.588)	(1.389)	(4.590)	(1.383)	(4.592)	(1.377)	(4.598)	(1.360)	(4.605)	(1.340)
H_6-O_3	2.342	2.440	2.344	2.442	2.346	2.439	2.354	2.428	2.363	2.420
	(2.321)	(2.392)	(2.323)	(2.395)	(2.325)	(2.394)	(2.333)	(2.389)	(2.341)	(2.397)
Bond angle										
$O_2S_1O_3$	108.9	108.8	108.6	108.7	108.6	108.6	108.3	108.4	108.0	108.0
	(108.5)	(107.8)	(108.5)	(107.8)	(108.4)	(107.7)	(108.1)	(107.5)	(107.9)	(108.7)
$N_4O_3S_1$	108.5	120.1	108.5	120.0	108.6	120.0	108.5	120.1	108.6	120.1
	(106.7)	(118.8)	(106.8)	(118.8)	(106.8)	(118.9)	(106.8)	(119.1)	(106.9)	(116.0)
$C_5N_4O_3$	109.2	107.0	109.4	107.2	109.5	107.2	109.8	107.3	110.3	107.5
	(108.0)	(109.6)	(108.2)	(109.7)	(108.3)	(109.7)	(108.6)	(109.8)	(109.0)	(109.4)
$H_6C_5N_4$	120.7	112.7	120.8	112.8	120.9	112.8	121.1	112.6	121.4	112.5
	(120.3)	(110.6)	(120.3)	(110.7)	(120.4)	(110.7)	(120.7)	(110.7)	(120.9)	(111.3)
Dihedral angle										
$O_2S_1O_3N_4$	-67.1	27.3	-67.1	27.1	-67.1	26.9	-66.9	26.6	-66.8	26.2
	(-67.2)	(30.6)	(-67.2)	(30.4)	(-67.2)	(30.3)	(-67.0)	(30.1)	(-66.9)	(36.7)
$S_1O_3N_4C_5$	180.1	-21.0	180.1	-20.6	180.0	-20.5	180.0	-20.1	180.0	-19.8
	(179.9)	(-23.6)	(180.1)	(-23.2)	(180.1)	(-23.1)	(180.0)	(-23.0)	(180.0)	(-27.6)
$O_3N_4C_5H_6$	0.0	3.6	0.0	3.5	0.0	3.5	0.0	3.5	0.0	3.5
	(0.0)	(4.5)	(0.0)	(4.3)	(0.0)	(4.3)	(0.0)	(4.4)	(0.0)	(5.5)

[a]bond lengths in Å, bond angles in degrees. [b]ONIOM (MP2) values are shown in parentheses.

four-membered ring transition state in which H_6 atom attacks on O_3 atom. We used HF/3-21G and ONIOM (DFT) methods to locate both the four-membered ring and the six-membered cyclic transition states. The predicted activation barriers of the four-membered ring TS are 18.30 and 17.59 kcal/mol higher than those of the six-membered ring TS at HF/3-21G and ONIOM (DFT) levels of theory, respectively, indicating the former can not compete with the latter. Thus we conclude that the thermal elimination of oximes proceeds through a six-membered cyclic TS rather than a four-membered ring TS.

For the six-membered ring TS, the ONIOM (DFT) optimized distance between atoms O_2 and H_6 is in the range of 1.43-1.51 Å, becoming much shorter by about 3.15 Å than its length in the reactant, still not being close to that in the product (*ca.* 0.97 Å). The bond lengths of the broken bonds (O_3-N_4 and C_5-H_6 bonds) lengthen significantly (1.99-2.03 Å for O_3-N_4 bond and 1.17-1.19 Å for C_5-H_6 bond, respectively). The ONIOM (MP2) TSs displays shorter O_3-N_4, N_4=C_5, O_2-H_6 bond lengths and longer S_1-O_3 and C_5-H_6 bond lengths than those in the corresponding ONIOM (DFT) structures.

In Table 2, the NBO charges of the relevant atoms and groups in reactant, transition state, and products of oxime (Y=H) as well as their changes in activation process and reaction equilibrium are listed. Upon going from reactant to TS, the charge on O_3 atom becomes more negative and the largely positive charge develops on N_4 atom, indicating the significant extent of polarization of the bond O_3-N_4 increases.

Bond Order Analysis. Bond order analysis can be used to gain further insight on the extent of bond formation or bond breaking along the reaction pathway.[13-15] An useful concept, synchronicity (*Sy*), proposed by Moyano *et al.*,[16] represents

Table 2. NBO charges of atoms and groups and the changes of charges, $\Delta q^{\neq}$ and Δq° involved in activation and equilibrium processes for oxime (Y=H) at ONIOM (B3LYP) and ONIOM (MP2) levels (in electronic charge unit)[a,b]

	RE	TS	PR	$\Delta q^{\neq}$	Δq°
$S_1(O_7)$	1.470	1.468	1.478	-0.002	0.008
	(1.477)	(1.483)	(1.488)	(0.006)	(0.018)
O_2	-0.937	-0.987	-0.884	-0.050	0.053
	(-0.940)	(-0.978)	(-0.887)	(-0.038)	(0.053)
O_3	-0.618	-0.911	-0.968	-0.293	-0.350
	(-0.621)	(-0.872)	(-0.971)	(-0.251)	(-0.350)
N_4	-0.178	0.086	-0.304	0.264	-0.126
	(-0.182)	(0.032)	(-0.303)	(0.214)	(-0.121)
C_5	0.120	0.015	0.288	-0.105	0.168
	(0.126)	(0.004)	(0.287)	(-0.122)	(0.161)
H_6	0.235	0.385	0.493	0.150	0.258
	(0.237)	(0.392)	(0.494)	(0.155)	(0.257)
X-ring	-0.105	-0.157	-0.099	-0.052	0.006
	(-0.112)	(-0.146)	(-0.124)	(-0.034)	(-0.012)
Y-ring	0.012	0.102	-0.005	0.090	-0.017
	(0.014)	(0.086)	(0.016)	(0.072)	(0.002)

[a]$\Delta q^{\neq} = q^{(TS)} - q^{(RE)}$, $\Delta q^{\circ} = q^{(PR)} - q^{(RE)}$. [b]ONIOM (MP2) charges are shown in parentheses.

the global nature of bond breaking/forming processes in the decomposition reaction and is given by Eq. (2).

$$Sy = 1 - \frac{\sum_{i=1}^{n} \frac{|(\%Ev)_i - (\%Ev)_{av}|}{(\%Ev)_{av}}}{2n-2} \quad (2)$$

Where n denotes the number of bonds directly involved in the reaction, $(\%Ev)_i$ and $(\%Ev)_{av}$ are the percentage of bond order evolution of bond i and the average value of all $(\%Ev)_i$, respectively. The percentage of evolution of the bond order is expressed:

$$(\%Ev)_i = \frac{(BO)_i^{TS} - (BO)_i^{RE}}{(BO)_i^{PR} - (BO)_i^{RE}} \times 100 \quad (3)$$

In Eq. (3) the superscripts TS, RE, and PR refer to the transition state, reactant, and product, respectively. $(BO)_i$ is the bond order defined according to the Pauling expression:[17]

$$(BO)_i^{SP} = \exp\left(\frac{r_i(1) - r_i(SP)}{0.3}\right) \quad (4)$$

Where $r_i(SP)$ is the length of bond i at the stationary point (SP) and $r_i(1)$ is the reference bond length. We show in Table 3 the relevant percentages of evolution of bond order ($\%Ev$) and synchronicities (Sy) for oximes (Y = OCH_3, CH_3, H, Cl, NO_2).

From Table 3, the $\%Ev$ values suggest that the O_3-N_4 bond-breaking is most advanced among all bond-breaking/forming processes, which is accompanied by further polarization of O_3-N_4 bond reflected by the charge development across the bond. The S_1-O_3 bond changing from single bond to double bond is also advanced ($\%Ev$: 63.26-64.24% for ONIOM (DFT) and 57.70-59.75% for ONIOM (MP2)). However, the C_5-H_6 bond-breaking and O_2-H_6 bond-forming are very late, which correspond to the H_6 atom transfer from C_5 to O_2 atom. The synchronicity of 0.7 (ONIOM (DFT)) or 0.8 (ONIOM (MP2)) shows that the pyrolysis of sulphonyl oximes is very asynchronous concerted process.

Table 3. Percentage of evolution of bond order ($\%Ev$) and synchronicity (Sy) for the pyrolysis reactions at ONIOM (DFT) and ONIOM (MP2)[a] levels of theory

Y	OCH_3	CH_3	H	Cl	NO_2
$S_1 = O_2$	37.60	38.19	38.79	40.57	42.74
	(40.24)	(40.34)	(41.38)	(41.98)	(44.36)
S_1-O_3	63.26	63.37	63.59	63.83	64.24
	(57.70)	(57.94)	(57.70)	(57.84)	(59.75)
O_3-N_4	86.38	86.33	86.24	85.87	85.44
	(79.47)	(79.33)	(79.20)	(78.70)	(80.01)
%Ev $N_4 = C_5$	29.72	32.17	32.51	32.51	34.53
	(51.72)	(52.83)	(52.83)	(53.43)	(56.40)
C_5-H_6	22.12	23.15	24.17	26.41	29.06
	(32.97)	(33.86)	(34.30)	(35.81)	(39.35)
O_2-H_6	16.81	17.44	18.09	19.72	21.87
	(24.84)	(25.33)	(25.84)	(27.34)	(29.23)
Sy	0.698	0.711	0.717	0.732	0.754
	(0.814)	(0.812)	(0.818)	(0.830)	(0.838)

[a]ONIOM (MP2) values are shown in parentheses.

As one can see from Scheme 1, the transition state involves the changes of the three bonds, (a), (b), and (c). In fact, any one of the bonds (a), (b), and (c) could be the prime contributor to molecular reactivity, or the electronic synergism of two or all of the three bonds determines the overall reactivity. From the bond order analysis above we may reasonably draw a conclusion that the reaction rate in the thermal decomposition of oximes is dominated by the polarity of O_3-N_4 bond (a), rather than the protophilicity of bond (b) or the H-bond donor acidity of (c).

Energetics. The activation and equilibrium parameters obtained by HF/3-21G and ONIOM levels for the thermal elimination of tosyl arenecarboxldoximes (Y = OCH_3, CH_3, H, Cl, and NO_2) are listed in Table 4 together with the experimental Arrhenius activation energies and rates.[2]

The decompositions of oximes are exothermic processes with negative ΔE° values at all levels of theory. The reaction free energy changes are also negative. The predicted activation energies are strongly dependent on the computational levels, but the tendencies in both methods from Y=OCH_3 to Y=NO_2 are well reproduced, *i.e.*, $\Delta E^{\neq}$ and E_a values increase in the same order of OCH_3 < CH_3 < H < Cl < NO_2. The experimental activation energies listed in Table 4 vary in the range of 23-25 kcal/mol but did not show such trend as found for the theoretical activation energies due to the relatively large experimental errors (maximum error was ±0.43 kcal/mol). Nevertheless, the magnitude of these experimental energies can be used to judge the quality of the two ONIOM methods. Comparing the calculated activation energies E_a with the experimental values, it is found that HF/3-21G and ONIOM (MP2) methods overestimate them by

Table 4. Activation and equilibrium parameters of the pyrolysis of oximes (Y=OCH_3, CH_3, H, Cl, and NO_2) at HF/3-21G, ONIOM (DFT) and ONIOM (MP2) levels of theory; experimental activation energies and rates (at 380 K and 1 atm)[a]

Y	Method	Calculated						Observed[c]	
		$\Delta E^{\neq}$ [b]	$\Delta S^{\neq}$	E_a	ΔE° [b]	ΔS°	ΔG°	E_a	$10^3 k$
OCH_3	HF	33.14	-2.45	33.78	-37.59	39.74	-52.60	23.36 ± 0.29	2.53
	ONIOM(DFT)	20.63	-5.05	22.97	-29.77	37.55	-44.06		
	ONIOM(MP2)	34.17	-4.76	34.55	-40.50	37.66	-54.83		
CH_3	HF	33.70	-1.67	34.36	-37.56	40.95	-53.00	24.26 ± 0.43	4.44
	ONIOM(DFT)	23.37	-4.15	23.74	-29.69	38.77	-44.41		
	ONIOM(MP2)	34.81	-3.88	35.22	-40.43	38.91	-55.20		
H	HF	34.03	-1.97	34.69	-37.49	39.63	-52.44	23.48 ± 0.32	2.60
	ONIOM(DFT)	23.94	-4.49	24.31	-29.56	37.49	-43.80		
	ONIOM(MP2)	35.26	-4.22	35.66	-40.31	37.64	-54.60		
Cl	HF	34.82	-1.72	35.48	-36.82	39.67	-51.81	23.31 ± 0.43	1.80
	ONIOM(DFT)	25.52	-4.45	25.89	-28.67	37.48	-42.95		
	ONIOM(MP2)	36.51	-4.00	36.91	-39.45	37.66	-53.78		
NO_2	HF	35.80	-0.48	36.50	-36.13	39.70	-51.14	–	–
	ONIOM(DFT)	27.52	-3.80	27.94	-27.70	37.50	-42.00		
	ONIOM(MP2)	37.18	-3.72	37.57	-38.52	37.73	-52.89		

[a] $\Delta E^{\neq}$, ΔE°, ΔG°, and E_a in kcal/mol; $\Delta S^{\neq}$ and ΔS° in cal/(mol.K); k in s^{-1}. [b] Zero-point vibrational energy included. [c] Taken from Ref. [2].

10-12 kcal/mol due to the inherent inaccuracy of the Hartree-Fock method. For ONIOM (DFT) level, the theoretical activation energies of 22.97-27.94 kcal/mol are in excellent agreement with the experimental values with the average deviation of 1.08 kcal/mol. In our previous work,[18] it has been shown that the combination of two non-empirical methods to an two-layered ONIOM model can reproduce the $\Delta E^{\neq}$ and E_a values accurately in comparison with the experimental results.

Substituent Effect. Polar substituent effects are investigated extensively in kinetic investigations of reaction mechanism. In this work, several substituents Y=OCH_3, CH_3, H, Cl, NO_2, are chosen at the para position in the Y-phenyl rings. We take a series of oximes as an example to study the effect of the substituents of Y-ring on the reactivity and properties of molecules. The above energy calculation and energetic analysis have indicated that the activation energy E_a decreases and the rate constant increases for the pyrolysis of oximes when the Y-substituent becomes more electron-donating. This is due to the fact that the electron-donating substituent transmits its effect, through the conjugated structure of the aromatic Y-ring and C_5=N_4 bond, to the reaction center N_4 atom, developing a positive charge on going from reactant to transition state (see Table 2). The effects of Y-ring substituents on the O_3-N_4 distances of the RE and TS are also seen in Table 1. The presence of an electron donating group at the para position of Y-ring leads to lengthening of O_3-N_4 bond along the reaction coordinate compared to that of Y=H. The greater the electron donating power, the more the change of bond length is. The substitution of Y-ring by electron-withdrawing group has the opposite effect on the O_3-N_4 distance. The trend of bond length changes is consistent with that of polarity change of this bond. As the Y group changes from electron-withdrawing to electron-donating, exothermicity of reaction becomes more negative (see Table 4) and the products are more stabilized. According to the Hammond postulate,[19] TS structure is shifted to "earlier" position and is more reactant-like, as we have seen from the %*Ev* values of C_5-H_6 bond (22.12% for Y=OCH_3 *vs.* 29.06% for Y=NO_2) and O_2-H_6 bond (16.81% for Y=OCH_3 *vs.* 21.87% for Y=NO_2) for ONIOM (DFT) method. Similar trend is also found for ONIOM (MP2) results.

For oximes, all Gibbs free energy changes from reactant to transition state, calculated by HF/3-21G and ONIOM methods are given in Table 5. The Hammett linear free energy

Table 5. Free energy changes of various Y-substituted tosyl arenecarboxaldoximes for activation process[a]

Y	σ	HF		ONIOM (DFT)		ONIOM (MP2)	
		$\Delta G^{\neq}$	$-\Delta G^{\neq}/(2.303RT)$	$\Delta G^{\neq}$	$-\Delta G^{\neq}/(2.303RT)$	$\Delta G^{\neq}$	$-\Delta G^{\neq}/(2.303RT)$
OCH_3	-0.27	33.95	-19.53	24.13	-13.88	35.60	-20.47
CH_3	-0.17	34.24	-19.70	24.56	-14.13	35.93	-20.66
H	0.00	34.68	-19.95	25.26	-14.53	36.51	-21.00
Cl	0.23	35.38	-20.36	26.83	-15.43	37.67	-21.66
NO_2	0.78	35.93	-20.67	28.62	-16.47	38.22	-21.98
ρ_y		-1.09 (r = 0.967)		-2.52 (r = 0.991)		-1.47 (r = 0.952)	

[a] $\Delta G^{\neq}$ in kcal/mol.

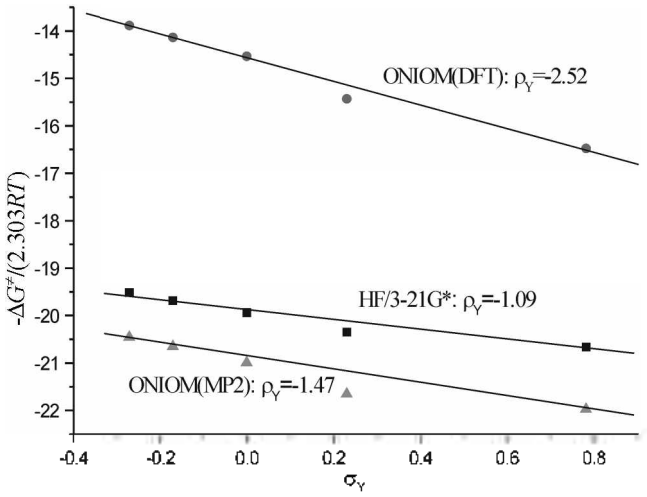

Figure 2. Hammett plots of $-\Delta G^{\neq}/(2.303RT)$ *vs* σ_Y for the activation process of pyrolysis of oximes at HF, ONIOM (DFT), and ONIOM (MP2) levels.

relationship correlating rate constant with electronic property of substituent. σ. is expressed by Eq. (5):

$$-\Delta G^{\neq}/(2.303RT) = \rho\,\sigma + c \qquad (5)$$

The simple ρ_Y values derived from the slope of Eq. (5) (see Fig. 2) are also listed in Table 5. From Table 5. one can see that the magnitude of Hammett ρ_Y value is strongly dependent on the computational level. The Hammett plot for the experimental results did not show any linearity (no experimental ρ_Y value was available) because of relatively large errors in the activation energies as mentioned above. Careful reexamination of the experimental work may be required. since we found fairly good linear correlations ($r \geq 0.95$) for all three computational works. Nevertheless. considering the accuracy of the activation energies. the ρ_Y value obtained by ONIOM (DFT) method could be more correct than the other ρ_Y values.

Conclusion

The thermal decomposition of sulphonyl oximes in gas phase has been theoretically studied using HF/3-21G and ONIOM methods. From the transition state structure and bond order analysis. this reaction is confirmed to be a concerted asynchronous process *via* a six-membered ring transition state. The calculated Arrhenius activation energies obtained at ONIOM (DFT) level of theory are in very good agreement with the observed ones for oximes with substituents p-OCH_3. p-CH_3. H. p-Cl. and p-NO_2 on Y-ring. The reactions of all molecules under study are exothermic. It is predicted that the electron-donating Y substituent may increase the reaction constant of the reaction. We suggest that further experiments may be carried out to verify our theoretical works.

Acknowledgements. This work was supported by Korea Research Foundation Grant (KRF-2000-015-DP0208).

References

1. Al-Awadi. N. A.; Elnagdi. M. H.; Kaul, K.; Ilingovan. S.: El-Dusouqni. O. M. E. *Tethahedron* **1998**. *54*. 4633.
2. Al-Awadi. N. A.; Elnagdi. M. H.; Kaul, K.; Ilingovan. S.: El-Dusouqni. O. M. E. *J. Phys. Org. Chem.* **1999**. *12*. 654.
3. Al-Awadi. N. A.: Elnagdi. M. H.: Al-Awadhi. H. A.: El-Dusouqni. O. M. E. *Int. J. Chem. Kinet.* **1998**. *30*. 457.
4. Al-Awadi. N. A.; El-Dusouqni, O. M. E.: Mathew. T. *Int. J. Chem. Kinet.* **1997**. *29*. 289.
5. Al-Awadi. N. A.: Elnagdi, M. H.; Mathew. T.: El-Gamry, I.; Khalik. M. A. *Int. J. Chem. Kinet.* **1996**. *28*. 741.
6. Dapprich. S.: Komaromi. I.: Byun. K. S.: Morokuma. K.: Frisch. M. J. *J. Mol. Struct. (THEOCHEM)* **1999**. *461*. 1.
7. Vreven. T.: Morokuma. K. *J. Comput. Chem.* **2000**. *21*. 1419.
8. Becke. A. D. *J. Chem. Phys.* **1993**. *98*. 5648.
9. Lee. S.; Yang. W.: Parr. R. G. *Phys. Rev.* **1988**. *B37*. 785.
10. Hehre. W. J.; Ditchfield. R. D.: Pople. J. A. *J. Chem. Phys* **1972**. *56*. 2257.
11. Frisch. M. J.; Trucks. G. W.; Schlegel. H. B.; Scuseria. G. E.; Robb. M. A.; Cheeseman. J. R.; Zakrzewski. V. G.; Montgomery. J. A.. Jr.; Stratmann. R. E.; Burant. J. C.; Dapprich. S.; Millam. J. M.; Daniels. A. D.; Kudin. K. N.; Strain. M. C.; Farkas. O.; Tomasi. J.; Barone. V.; Cossi. M.; Cammi. R.; Mennucci. B.; Pomelli. C.; Adamo. C.; Clifford. S.; Ochterski. J.; Petersson. G. A.; Ayala. P. Y.; Cui. Q.; Morokuma. K.; Malick. D. K.; Rabuck. A. D.; Raghavachari. K.; Foresman. J. B.; Cioslowski. J.; Ortiz. J. V.; Stefanov. B. B.; Liu. G.; Liashenko. A.; Piskorz. P.; Komaromi. I.; Gomperts. R.; Martin. R. L.; Fox. D. J.; Keith. T.; Al-Laham. M. A.; Peng. C. Y.; Nanayakkara. A.; Gonzalez. C.; Challacombe. M.; Gill. P. M. W.; Johnson. B.; Chen. W.; Wong. M. W.; Andres. J. L.; Gonzalez. C.; Head-Gordon. M.; Replogle. E. S.; Pople. J. A. *Gaussian 98. Revision A.7*. Gaussian Inc.: Pittsburgh PA. 1998.
12. Fukui. K. *J. Phys. Chem.* **1970**. *74*. 4161.
13. Varandas. A. J. C.: Formosinho. S. J. F. *J. Chem. Soc. Faraday Trans.* **1986**. *2*. 282.
14. Rotinov. A.: Chuchani. G.: Andres. J.: Domingo. L. R.: Safont. V. S. *Chem. Phys.* **1999**. *246*. 1.
15. Lim. C. C.: Xu. Z. P.: Huang. H. H.: Mok. C. Y.: Chin. W. S. *Chem. Phys. Lett.* **2000**. *325*. 433.
16. Moyano. A.; Pericas. M. A.: Valenti. A. *J. Org. Chem.* **1989**. *54*. 573.
17. Pauling. L. *J. Am. Chem. Soc.* **1947**. *69*. 542.
18. Xue. Y.: Kang. C. H. : Kim. C. K.: Lee. I. *J. Comput. Chem.* **2003**. *24*. 963.
19. Dewar. M. J. S.: Dougherty. R. C. *The PMO Theory of Organic Chemistry*. Plenum Press: New York. 1975: p 219.